

RAG-Driver: Generalisable Driving Explanations with Retrieval-Augmented In-Context Learning in Multi-Modal Large Language Model

Jianhao Yuan¹, Shuyang Sun¹, Daniel Omeiza¹, Bo Zhao², Paul Newman¹, Lars Kunze¹, Matthew Gadd¹

¹ University of Oxford ²Beijing Academy of Artificial Intelligence

{jianhaoyuan, kevinsun, daniel, pnewman, lars, mattgadd}@robots.ox.ac.uk

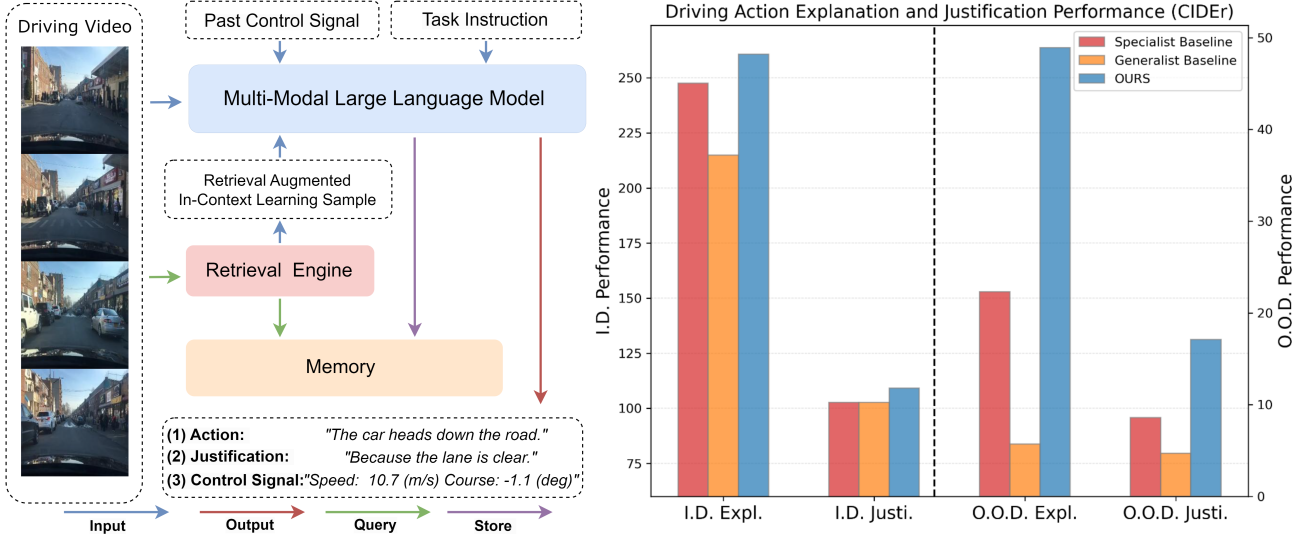


Fig. 1: **Left:** In natural language, our system describes *and* justifies actions taken by the vehicle, as well as infers the driving action in the form of numerical control signals (speed, and steering angle). For this, we use a unified perception and planning module through a Multi-modal Large Language Model. Our core contribution is a *retrieval mechanism* to search driving scenarios similar to the current condition and use these to augment the current predictions through In-Context Learning. This leads to better overall description and prediction and is more generalisable in new deployment domains. **Right:** Comparison between our methods and baselines for the in-distribution (I.D., left vertical axis) and out-of-distribution (O.O.D., right vertical axis) generalisation settings as specified in Sec. IV. Note that I.D. Performance and O.O.D. Performance have different vertical scales. Despite the performance gap between these two settings our method significantly outperforms all of the baselines, including the specialist baseline, ADAPT [35], as well as the generalist baseline, DriveGPT4 [81], in terms of driving action explanation (Expl. on the horizontal axis) and justification (Justi. on the horizontal axis) tasks, as measured by CIDEr..

Abstract—We need to trust robots that use often opaque AI methods. They need to explain themselves to us, and we need to trust their explanation. In this regard, explainability plays a critical role in trustworthy autonomous decision-making to foster transparency and acceptance among end users, especially in complex autonomous driving. Recent advancements in Multi-Modal Large Language models (MLLMs) have shown promising potential in enhancing the explainability as a driving agent by producing control predictions along with natural language explanations. However, severe data scarcity due to expensive annotation costs and significant domain gaps between different datasets makes the development of a robust and generalisable system an extremely challenging task. Moreover, the prohibitively expensive training requirements of MLLM and the unsolved problem of catastrophic forgetting further limit their generalisability post-deployment. To address these challenges, we present *RAG-Driver*, a novel retrieval-augmented multi-modal large language model that leverages in-context learning for high-performance, explainable, and generalisable autonomous driving. By grounding

in retrieved expert demonstration, we empirically validate that *RAG-Driver* achieves state-of-the-art performance in producing driving action explanations, justifications, and control signal prediction. More importantly, it exhibits exceptional zero-shot generalisation capabilities to unseen environments without further training endeavours.

Index Terms—Autonomous driving, multi-modal language model, end-to-end driving, domain generalisation

I. INTRODUCTION

Driven by the emerging development of deep learning, autonomous driving has observed a paradigm shift from rules-based decision systems [66, 21] to data-driven learning-based approaches [30, 6, 37]. However, this comes at the cost of transparency in decision-making, especially for end-to-end autonomous driving systems which are considered black-box in nature [13]. Thus, in addition to precision in action control,

explanation provision is key to ensuring trustworthy decision-making to reconcile the system’s decisions with end-user expectations to foster confidence and acceptance [82, 8] in dynamic driving environments.

Traditional approaches have mainly relied on attention visualisation [5, 7, 55] as a proxy to rationalise the decisions of the black-box systems or auxiliary intermediate tasks such as semantic segmentation [26, 34], object detection [16, 33], and affordance prediction [68, 45] provide meaningful intermediate representation for decision-making. However, these methods do not engage end-users in the dialogue as they are one-directional and not readily comprehensible by the general users for the purpose of fostering trust and confidence. An alternative promising approach is the integration of natural language explanations [39, 35, 54], in particular through Multi-Modal Large Language Models (MLLMs) [1, 71]. These models, pre-trained on extensive web-scale datasets, demonstrate remarkable reasoning capacity, enabling the transformation of complex vehicular decision-making processes into more understandable narrative formats, thereby offering a new layer of explainability to conventional systems.

While several early attempts have demonstrated the potential of MLLMs as general explainable driving agents [81, 78, 51], these methods fall short of human-level understanding. One of the limitations is their failure to generalise to unseen environments. A primary obstacle is the lack of high-quality annotated data [56], coupled with the significant domain shift across various datasets [24], which hinders the model’s generalisation capacity to novel environments outside of the training data distribution. Another critical challenge is the prohibitively expensive training requirement and the unsolved problem of catastrophic forgetting [40], which make re-training or fine-tuning impractical solutions due to the immense computational demands and severe performance degradation. Consequently, this further limits the models’ generalisability after deployment, as they struggle to effectively utilise new data in constantly evolving environments and driving scenarios.

To address these challenges, we introduce *RAG-Driver*, a novel retrieval-augmented multi-modal large language model tailored for generalisable and explainable end-to-end driving. As illustrated in Fig. 1, it outputs natural language texts corresponding to (1) the driving action and (2) justification of that driving action along with (3) numerical control signals based on driving videos. Action and justification text accuracy, on the right, are much improved by our method (note that, for visualisation, in-distribution and out-of-distribution Performance have different vertical scales, with the latter being a much more difficult task). The natural language texts are also aligned with control signals during in-context learning [10] to enable faithful introspective explanation provision. The novelty of *RAG-Driver* is the integration of retrieval-augmented in-context learning (RA-ICL) mechanisms that significantly improve generalisation performance in unseen driving environments. It allows efficient recall of similar driving scenarios as contextual information augmenting MLLM prediction through implicit meta-optimisation (Sec. III-C). Through extensive experiments,

we show that *RAG-Driver* outperforms existing methods on both in-domain deployments as well as deployment in unseen environments (without any fine-tuning). By being grounded in analogical demonstrations, our framework significantly reduces the need for continuous retraining while enhancing the generalisability and quality of generated explanatory texts. Our primary contributions are as follows:

- 1) Proposing a novel retrieval-augmented in-context learning method for Multi-Modal Large Language Model (MLLM) based generalisable and explainable driving.
- 2) Achieving state-of-the-art introspective driving explanation performance on the standard benchmark BDD-X [39].
- 3) Demonstrating exceptional zero-shot generalisation capacity to unseen scenarios without training effort through a customised dataset *Spoken-SAX* featuring video sequences narrated by a professional driving instructor.

II. RELATED WORK

A. Explainable End-to-End Autonomous Driving

End-to-end learned driving [13] maps directly from raw sensor input to vehicle control signals. This data-driven, joint optimisation of perception, prediction, and planning can be simple and efficient [30]. In this area, various learning-based approaches, including behavior cloning [6, 12, 61, 86, 60], inverse optimal control [84, 65, 77], and reinforcement learning [37, 73, 11, 44] are promising. A key area of focus in this area is explainability [83], which is crucial for improving transparency and building trust towards wider public acceptance of autonomous systems [? 57]. One line of works leverages attention visualisation – either to directly identify salient regions of input images that are important for driving decision-making [38, 5, 7] or to assist feature aggregation for downstream motion planning tasks [55, 15, 80, 63]. Another line of work uses intermediate auxiliary tasks such as semantic segmentation [26, 34], object detection [16, 33], and affordance prediction [68, 45] which help to decode latent representations to human-understandable representation. While these methods provide explainable mechanisms by associating decision-making processes with semantic or visual representations, they are not readily comprehensible by the general users for the purpose of fostering trust and confidence.

Alternatively, recent research shows promise in utilising natural language explanation. Several works develop specialist explainers [39] using attention alignment in visual input and textual generation for grounded driving action explanation. ADAPT [35] uses a vision-language transformer with separate decoder for caption generation alongside control signal prediction. More recently, several works explore the potential of Multi-modal Large Language Models (MLLMs). Works such as, DriveGPT4 [81], Lingo [54], and DrivingMLM [78] have shown promising potential in general question-answering for driving and action planning. However, a common obstacle in both specialist and MLLM-based generalist models is the scarcity of data due to expensive annotation costs and

significant domain gaps between different datasets, making the development of a robust and generalisable model an extremely challenging task. In our work, we aim to overcome these obstacles by employing a more robust inference paradigm of retrieval-augmented in-context learning to bridge domain gaps and circumvent the need for annotations in new domains.

B. Multi-Modal Large Language Model

Recent advancements in Large Language Models (LLMs) have paved the way for the emergence of Multi-modal Large Language Models (MLLMs) [1, 71, 3, 48, 89, 43, 27, 46, 85]. Benefiting from scalable transformer-based architecture and web-scale training data, these models have demonstrated notable capabilities in general-purpose visual understanding tasks. One line of work focuses on modality fusion in the latent space, offering a scalable, end-to-end solution for MLLMs. For instance, Flamingo [3] and BLIP2 [43] fuse visual tokens to frozen LLM through gated attention and query transformers, respectively. LLaVA [48] and MiniGPT4 [89] use simple Multi-Layer Perceptron (MLP) with visual instruction tuning to align the pre-trained image encoder to LLM. Most relevant to us is the line of work focusing on video-language models such as Video-LLaVA [46] and Video-LLaMA [85], which integrate pre-trained video encoders into LLMs using strategies similar to those in image-based models.

With remarkable perception and reasoning capacity, MLLMs reveal promising potential in various robotics tasks such as reasoning [20, 2, 32] and planning [62, 9, 47]. The most similar to us is the idea that engages a generalist foundation model for end-to-end embodied agent. PaLM-e [20] injects images, state estimates, and other sensor modalities to LLM and autoregressively produces natural language commands. RT-2 [9] and RT-X [58] fine-tune on image and low-level robot control signal pairs to perform end-to-end robot control. Specifically in driving, numerous approaches leverage language-only LLMs for decision-making [82] and then augment it with external perception module feedback [53, 25, 14], designed chain-of-thought reasoning templates [53, 52] or downstream planning [67, 69, 14] to form a system-level driving agent. Another more relevant line of work is end-to-end driving agents. DriveGPT4 [81] leverages a fine-tuned video-language model Valley [50] on driving specific visual instruction tuning based on BDD-X [39]. Dolphins [51] further use the designed Grounded chain-of-thought to enhance reasoning capacity. DrivingMLM [78] and Reason2Drive [56] scale up the driving visual instruction tuning dataset through simulator-based data engine and annotation of existing large-scale datasets, respectively. While these approaches have demonstrated the potentials of MLLM, the prohibitively expensive training cost and the unsolved problem of catastrophic forgetting, which makes re-training or fine-tuning post-deployment challenging, further limiting their generalisation capacity to unseen driving environments. To solve this problem, we leverage a training-free retrieval-augmented in-context learning mechanism.

C. In-Context Learning and Retrieval-Augmented Generation

While LLMs demonstrate strong generative and reasoning capacity, there are still several issues associated with their output, such as hallucination [31], and slow knowledge updates [36]. In-context Learning (ICL) [10, 18] has emerged as a promising approach in LLM inference, potentially addressing several of these issues. This paradigm involves providing a test query alongside a few demonstration examples as contextual information. The LLM then generates an output for the test instance based on analogies drawn from context, without any updates to its parameters [64]. While ICL has been observed to enhance generalisability in various Natural Language Processing (NLP) tasks, its application in multi-modal contexts remains less explored, potentially due to the challenges associated with curating structured, high-quality multi-modal ICL datasets. Retrieval-Augmented Generation (RAG) [42] is another important inference paradigm for LLM. It provides an external knowledge database to augment the compressed knowledge within the LLM in inference by dynamically retrieving relevant information samples as contextual information. One of its promising applications is leveraging a systematic approach to curate In-Context Learning (ICL) examples. In this work, we build upon these inference paradigms and extend their application to Multimodal Large Language Models (MLLMs). We introduce a retrieval-augmented in-context learning mechanism through a curated multi-modal driving in-context instruction tuning dataset and a vector similarity-based retrieval engine specifically tailored for driving applications.

III. METHOD

RAG-Driver is a retrieval-augmented, multi-modal large language model (MLLM) for generalisable, explainable end-to-end driving. Its multi-tasking capabilities encompass three key areas: (1) Action Explanation, providing a human-understandable driving action description; (2) Action Justification, elucidating the rationale behind specific driving actions; and (3) Next Control Signal Prediction, forecasting upcoming control signals in response to the driving conditions. As shown in Fig. 2, it is composed of two primary components: a unified perception and planning unit built upon an MLLM backbone and a memory unit built upon a hybrid vector and textual database. These components interact through a retrieval engine, enabling robust multi-modal in-context learning (ICL) during decision-making.

A. Multi-modal Large Language Model Architecture

Following the successful MLLM paradigm of Video-LLaVA [46], we align visual and language embeddings through visual instruction tuning. We leverage a pre-trained video encoder and LLM and then inject the video embedding into the LLM through an MLP projector to build a fully differentiable MLLM.

Video Encoder We adopt the pre-trained LanguageBind video encoder [88] as our frozen visual backbone f_v , which is based on a ViT-B/32 vision transformer [19]. As shown in Fig. 3, given an input video frame sequence $V_i = \{v_i^1, v_i^2, \dots, v_i^k\} \in$

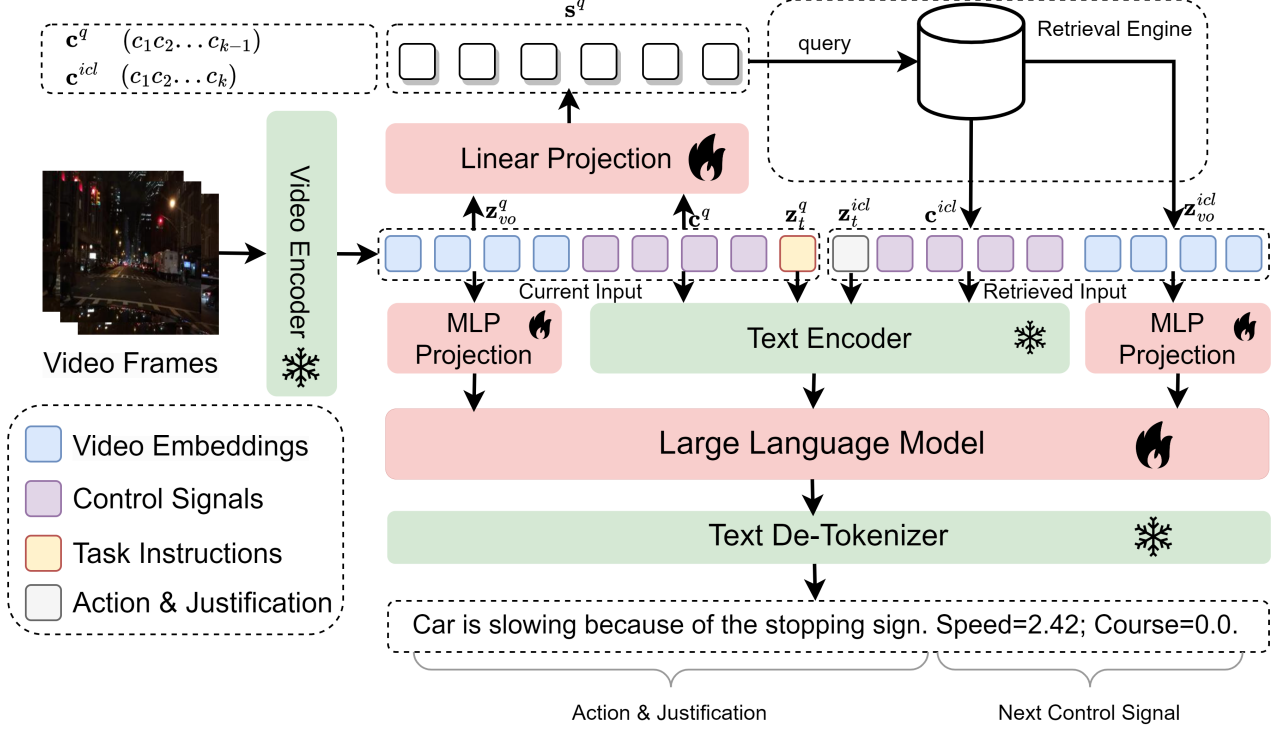


Fig. 2: **RAG-Driver Overview**: Given a query comprising a video of the current driving scenario and its corresponding control signal, the process starts with the input being fed into a Retrieval Engine. It searches within a memory database for driving experiences that are similar to the current scenario, thereby providing relevant In-context Learning (ICL) samples. Subsequently, a Multi-Modal Large Language Model (MLLM) processes both the current query and the retrieved in-context learning samples, where the encoded video embedding (z_{vo}^q or z_{vo}^{icl}) is further projected through a MLP to align it with the language embedding (z_t^q , z_t^{icl} , or c^{icl}) from the text encoder, so that the model can learn to associate relevant visual and textual features more effectively. Based on high-level task instructions, the model engages in various prediction tasks: Action Explanation, Action Justification, and Next Control Signal Prediction.

$\mathbb{R}^{3 \times k \times 224 \times 224}$, we first split the video into multiple temporal sequences, each consisting of patches that share the same spatial location across different frames. These patches are then transformed through a linear projection for a vision transformer to output video embedding $z_{vo} \in \mathbb{R}^{2048 \times 1024}$. The video encoder is pre-trained with video-language contrastive learning (i.e. CLIP4clip [49]) without further fine-tuning.

Cross-Modality Projector We then leverage a two-layer MLP to project and align the encoded video embedding z_{vo} with language token embeddings $z_v \in \mathbb{R}^{2048 \times 4096}$.

$$f_p(z_{vo}) = \text{GELU}(W_2 \cdot \text{GELU}(W_1 \cdot z_{vo})) \quad (1)$$

In particular, the projector f_p takes the form in Eq. (1), where we use GELU [28] as an activation function. We train the projector with a two-stage training strategy as detailed in Sec. III-B.

Large Language Model Backbone Finally, the LLM takes in both aligned video embedding z_v and language embedding z_t of textual context information and task instruction to predict both the textual action explanation and the numerical control signal. We adopt Vicuna 1.5 7B [87], which is instruction-tuned based on LLaMA2 [74] as our LLM backbone. For the decoder-

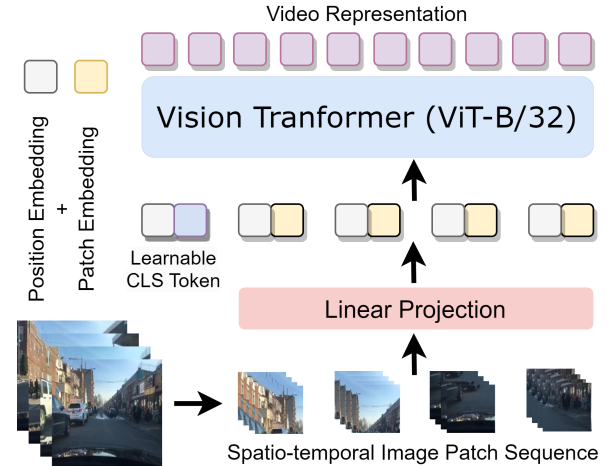


Fig. 3: **Video Encoder architecture**. Video is first split into $k \times 32 \times 32$ patches concatenated in time, where these patches are linear projected to video embedding. Then, the model is trained with video-language contrastive learning (CLIP4clip) [49] to obtain a language-aligned video representation.

only LLM conditioned on the multi-modal contextual prefix $\mathbf{z}_{1:n} = [\mathbf{z}_v, \mathbf{z}_t]$ of length N , the joint probability of the output $\mathbf{x}_{n+1:L}$ is as per Eq. (2), where P_θ is the transformer-based LLM backbone parameterized by θ .

$$P(\mathbf{x}_{n+1:L} | \mathbf{z}_{1:n}) = \prod_{l=n+1}^L P_\theta(\mathbf{x}_l | \mathbf{x}_{1:l-1}, \mathbf{z}_{1:n}) \quad (2)$$

Each output token \mathbf{x}_l is then sampled auto-regressively based on the previous output and context and finally decode to language space through a text de-tokenizer.

B. Training Strategy

Following the visual instruction tuning paradigm [48, 46], we employ a two-stage training strategy to progressively enable cross-modality alignment and multi-task driving capacity. In both stages, we leverage the same next-token prediction cross-entropy loss as in Eq. (3) aiming to maximize the conditional answer likelihood in Eq. (2), where \mathbf{y} is the ground truth token.

$$\mathcal{L}_{CE} = - \sum_{i=n+1}^L \mathbf{y}_i \log P(\mathbf{x}_i | \mathbf{z}_{1:n}) \quad (3)$$

Pre-training In the first pre-training stage, we only train the cross-modality projector while freezing the visual encoder and LLM. We use a subset of VIDAL-10M [88] which contains 3 million video-caption pairs. This achieves alignment between visual and language features by projecting the pre-trained video embeddings into language tokens understandable by LLM.

Instruction Tuning While state-of-the-art LLMs exhibit zero-shot ICL capability, several works [18] and our ablation study in Sec. IV-D have shown further improvement when specifically trained on curated ICL demonstrations. In particular, we construct a multi-modal instruction tuning dataset with structured ICL examples based on the BDD-X dataset [39] resulting in 16K video question and answer pairs. As shown in Fig. 4, for an 8-frame driving video sequence with associated control signals – speed, course, acceleration, and curvature as the current query, we retrieve two relevant driving experiences, which are then prefixed to the current query as ICL examples. The dataset is tailored to support three distinct tasks, each represented through question-answer pairs in natural language. Note that, with (1) Action Explanation and (2) Justification naturally represented as natural language, (3) Control Signal prediction is also formed as language token prediction; this is feasible due to the distinct mapping of numerical values to specific tokens within the language model dictionary.

C. Retrieval-Augmented In-context Learning

Another critical component of the system is the memory unit, which consists of a database and a retrieval engine. The database takes in a vectorised video embedding \mathbf{z}_{vo} , which is extracted with the same video encoder as in Sec. III-A, and control signals $\mathbf{c} \in \mathbb{R}^{28}$ directly from sensor recording. Each vector is uniquely associated with the corresponding human expert textual explanation and justification from training samples as in Sec. III-B.

Retrieval Mechanism To perform the retrieval, we first leverage a lightweight MLP projector of the same structure as in Eq. (1) to project the heterogeneous video and control signal embedding into the same hybrid embedding $\mathbf{s} \in \mathbb{R}^{1024}$ through metric learning [29]. In particular, we adopt a triplet loss with Euclidean distance as shown in Eq. (4):

$$\mathcal{L}_{Tri}(\mathbf{a}, \mathbf{p}, \mathbf{n}) = \max(||\mathbf{a} - \mathbf{p}||_2 - ||\mathbf{a} - \mathbf{n}||_2 + \text{margin}, 0) \quad (4)$$

where \mathbf{a} , \mathbf{p} , \mathbf{n} defines anchor, positive, and negative data sample, respectively. The positive (\mathbf{a}, \mathbf{p}) and negative pairs (\mathbf{n}, \mathbf{p}) between hybrid embedding \mathbf{s} are selected based on text similarity (i.e., TF-IDF Score) of the driving action and justification in the BDD-X training set. We aim to form the metric space such that the scenarios lead to similar driving actions close together and vice versa. This approach addresses the limitations of relying solely on visual similarity, which we have empirically found can result in sub-optimal performance (Sec. IV-D), and also solves the problem of heterogeneous sensor inputs that are difficult for similarity comparison. We then perform retrieval through an efficient vector similarity search. Given a query vector \mathbf{s}^q , the cosine similarity between the query vector and each vector in the database is computed as $S_c(\mathbf{s}_q, \mathbf{s}^{(i)}) = \frac{\mathbf{s}_q \cdot \mathbf{s}^{(i)}}{\|\mathbf{s}_q\| \|\mathbf{s}^{(i)}\|}$. Subsequently, we consistently select the two most relevant driving samples based on this similarity score. These samples represent the entire reasoning process, from contextual information to question-answer pairs, as illustrated in Fig. 4.

Retrieval Augmented In-Context Learning (RA-ICL) To perform the RA-ICL, we prefix these retrieved samples before the current query, facilitating an implicit gradient descent through the meta-optimiser of LLM, as proved in [17]. This approach is also applicable to MLLMs, with our MLLM architecture specified in Sec. III-A. For a given transformer-based pre-trained MLLM modeling the prefix-conditioned output probability as in Eq. (2), consider one head of the multi-head attention in a single transformer block as follows:

$$\begin{aligned} \mathcal{F}_{ICL}(\mathbf{z}_{1:n}) &= \text{Attention}(Q, K, V) \\ &= W_V [\mathbf{z}_{icl}; \mathbf{z}_q] \text{Softmax} \left(\frac{(W_K \mathbf{z}_{1:n})^T (W_Q \mathbf{z}_{1:n})}{\sqrt{d^i}} \right) \end{aligned} \quad (5)$$

where $\mathbf{z}_{1:n} = [\mathbf{z}_{icl}; \mathbf{z}_q]$ represents the ICL example \mathbf{z}_{icl} and current query embeddings \mathbf{z}_q , respectively. $W_{Q,K,V} \in \mathbb{R}^{d^i \times d^o}$ is the linear transformation on query, key, and value in the attention block, respectively. Now, in [17] in-context learning was shown to effectively achieve a meta-optimisation to implicitly update the model with an estimated meta-gradient. We provide in our work a new, alternative derivation of this, supported by more recent work in [41] on the following *softmax-free* linear attention expressions

$$\mathcal{F}_{ICL}(\mathbf{z}_{1:n}) = W_V [\mathbf{z}_{icl}; \mathbf{z}_q] (W_K [\mathbf{z}_{icl}; \mathbf{z}_q])^T W_Q \mathbf{z}_{1:n} \quad (6)$$

This can be simplified, with a more detailed derivation in Apx. C, as

$$\mathcal{F}_{ICL}(\mathbf{z}_{1:n}) = (\Delta W_{ICL} + W_{ZSL}) W_Q \mathbf{z}_{1:n} \quad (7)$$

Contextual System Information

A chat between a user and an assistant designed for autonomous driving. The assistant gives helpful, detailed, and polite answers to the user's questions including driving action justification and control signal based on current driving video.

In Context Learning Example 1:

Human: The video records a past driving scenario: <video>.

Control Signal until current Frame Sequence is:

Speed: [7.05, 9.68, 8.51, 4.56, 6.79, 6.62, 5.91].

Curvature: [0.0, 0.03, 0.0, 0.0, -0.0, -0.0, -0.0].

Acceleration: [1.17, 0.84, -2.56, 0.54, 0.24, -0.18, -0.83].

Course: [0.0, -3.86, 0.0, 0.0, 0.0, 0.0, 0.0].

What is the action of the ego car?

RAG-Driver: The car moves forward then comes to a stop.

Human: Why does the ego car do this?

RAG-Driver: Because traffic has stopped in front.

Further In Context Learning Examples in the Same Format

Current Query

Human: The video records the current driving scenario: <video>. Control Signal until current Frame Sequence is:

Speed: [8.38, 7.98, 6.92, 8.46, 10.09, 11.15, 10.35].

Curvature: [0.0, 0.0, 0.0, 0.0, -0.0, 0.0, -0.0].

Acceleration: [0.17, -0.67, 0.17, 0.54, 0.48, 0.57, -1.42].

Course: [0.0, 0.0, 0.0, 0.0, 0.73, 0.0, 0.0].

What is the action of the ego car?

RAG-Driver: *The car moves forward then comes to a stop.*

Human: Why does the ego car do this?

RAG-Driver: *Because traffic has stopped in front.*

Human: Predict the control signal of next frame

RAG-Driver: *Speed: 2.42 Course: 0.0*

Fig. 4: **Query Sample.** A single query includes three primary components: (1) Contextual System Information, a constant element across all queries that offers high-level task instruction; (2) Current Query, comprising all driving information and specific task instruction in natural language question-answer format. Driving video visual inputs (i.e. <video>) as represented here are in fact encoded video tokens from a video encoder and MLP projector which are concatenated with language tokens from a text encoder, see Fig. 2 for more architectural detail. Note that the red sentence is the expected output from MLLM; (3) Multiple In-Context Learning Examples, retrieved from memory, which serve as an analogical demonstration of a complete reasoning process—from sensor input in driving scenarios to action justification and control prediction.

where we separate out the terms W_{ZSL} independent of the ICL examples and dependent solely on the current query from those ΔW_{ICL} dependent on the ICL examples, given by:

$$\begin{aligned} \Delta W_{ICL} &= \sum_i W_V z_{icl,i} (W_K z_{icl,i})^T \\ W_{ZSL} &= W_V z_q (W_K z_q)^T \end{aligned} \quad (8)$$

Now, with more detail in Apx. C, a forward-pass

$$F(\mathbf{x}) = (W_0 + \Delta W)\mathbf{x} \quad (9)$$

through a linear layer F after its weights W_0 have been updated by ΔW has the weight updates coupled to the input in the form

$$\Delta W\mathbf{x} = \sum_i \eta \frac{\partial L}{\partial \mathbf{y}}|_{\mathbf{y}_i} \mathbf{x}_i^T \mathbf{x} \quad (10)$$

where $\mathbf{x}_i, \mathbf{y}_i$ are the (mini-batch) input and output to the layer that resulted in the weight update when backpropagating loss L and with learning rate η . Therefore we have a weighted sum of dot products, which is *akin to an attention mechanism*. Indeed, by inspection of similar dot-product expressions $W_V z_{icl,i} (W_K z_{icl,i})^T \leftrightarrow \eta \frac{\partial L}{\partial \mathbf{y}}|_{\mathbf{y}_i} \mathbf{x}_i^T \mathbf{x}$ we note that we match the form for the linear layer above

$$(W_{ZSL} + \Delta W_{ICL})W_{Qz1:n} \leftrightarrow (W + \Delta W)\mathbf{x}$$

This can therefore be interpreted to say that the output of the attention is adjusted in a meta-optimal way to conform to the samples provided as input context, much like gradient descent on the linear layer would adjust that layer to conform to the mini-batch training data, but *crucially* in the case of *RAG-Driver*, without backpropagation.

RA-ICL serves as an efficient inference method boosting the performance of MLLMs in explainable driving without further training effort, where we empirically verify it is extremely effective in boosting the model prediction performance and generalisation capacity.

IV. EXPERIMENTS

A. Settings and Datasets

We empirically evaluate the proposed framework of Retrieval-augmented In-Context Learning (RA-ICL) framework for Multi-modal Large Language Model (MLLMs), targeting explainable driving applications. We aim to validate its efficacy in general driving scenarios with a focus on two main aspects: (1) explainability in driving action explanation and justification. (2) Control Signal Prediction. We conduct experiments with the BDD-X [39] dataset, which is a widely adopted benchmark in explainable driving, comprising 77-hour videos across the US under different road and weather conditions. We customize the format as shown in Fig. 4, resulting in 16,803 and 2,123 video question-answering pairs for training and testing, respectively. More importantly, we further explore the transfer learning capacity of zero-shot generalisation in unseen environments. We leverage customised dataset comprising 58 testing question-answering pairs, recorded in London, UK as part of the Sense-Assess-eXplain dataset [22], presenting a significant distribution shift from the BDD-X dataset.

Benchmark Settings For all experiments, we train the MLLM using the BDD-X training split. Subsequent evaluation on general explainability and control signal prediction capabilities tests are conducted on the BDD-X test split with the BDD-X training split as the memory database. For the transfer learning

experiments, we employ the same foundational model and test it on the *Spoken-SAX* dataset but the memory database is constructed using the BDD-X training split for zero-shot generalisation.

Implementation Details for each of the driving videos, we uniformly sample the video to 8 frames and resize it to 224×224 for all frames. For MLLM, we train the model for one and two epochs in the pre-training and fine-tuning stages, respectively. For the embedding projector, we train the model for 300 epochs. Training of the retrieval engine on the BDD-X dataset using a single A100 GPU takes half an hour. Then, we utilize the pre-training checkpoint from Video-LLaVA [46] and fine-tune the MLLM on top of it, which takes 6 hours on 8 A100 GPUs. For the inference time, since we store all driving experience in a preprocessed database, which speeds up the retrieval process, the overall single round inference time is roughly 4 seconds on a single A100 GPU. Further experiment implementation details are provided in Apx. A.

Evaluation Metric For the driving action description and justification tasks, we use the same metrics as [35] including 4-gram BLEU (B4) [59], METEOR (M) [4], and CIDEr (C) [75]. These metrics aim to evaluate text generation quality, with BLEU focusing on n-gram precision, METEOR incorporating semantic and syntactic nuances, and CIDEr emphasising consensus and relevance in tasks like image captioning. Moreover, for the control signal evaluation, we again follow [35] and present Root Mean Square Error (RMSE) in both steering angle ($^{\circ}$) and speed (m s^{-1}). We also present “tolerant accuracy” metrics, A_{σ} , representing the accuracy of predictions when binarised as within a tolerance threshold σ of the ground truth.

Baselines We compare with various driving action description and justification baseline methods such as video-language sequence-to-sequence based recurrent neural network S2VT [76] and visual-attention based convolutional neural network WAA [39]. We also compare with a state-of-the-art video transformer-based driving action explanation method ADAPT [35]. Methods like this are specialist in that they use two branches for explanation and control signal prediction. Beyond these specialist models for driving explanation, we further compare with the generalist visual instruction-tuned MLLM, DriveGPT4 [81]. Generalist methods like this use the same backbone for explanation and control signal prediction.

B. Explainability in Driving Action and Justification

We begin by evaluating the quality and accuracy of explanations and justifications for driving actions separately. As shown in upper part of Tab. I, our method demonstrates comparable performance to the state-of-the-art specialist method ADAPT [35], a characteristic not observed in previous MLLM-based methods. In particular, when compared with DriveGPT4 [81] which also uses an MLLM with a similar architecture and number of parameters but incorporates the extra LLaVA-150K dataset [48] for visual instruction tuning, our approach, relying solely on the BDD-X dataset, outperforms it in terms of explainability. This is evidenced by an average performance improvement of 10.8% across all metrics. This

underscores the effectiveness of ICL in enhancing the emergent reasoning capabilities of MLLMs.

C. Control Signal Prediction

We next evaluate the accuracy of control signal predictions for Course (i.e., turning angle) and Speed. As indicated in Tab. II, our method surpasses others in open-loop control accuracy across various tolerance ranges and in terms of RMSE, significantly outperforming the baseline approach. In particular, when compared to the state-of-the-art DriveGPT4, which also uses the same visual input combined with past control signals for autoregressive prediction, our method stands out by implementing retrieval-augmented ICL examples. This indicates that the analogy in the overall reasoning process provided by the ICL examples also contributes to the improvement in numerical control signal prediction.

D. Ablation Study on Retrieval Strategy

We perform a more comprehensive ablation study to evaluate the efficacy of our proposed retrieval-augmented in-context learning. We first aim to investigate the similarity metric for retrieval. In particular, we compare the use of visual similarity (i.e., video embeddings only) with hybrid similarity (i.e., hybrid video and control signal projected embedding Sec. III-C). Our empirical findings indicate suboptimal performance when using visual similarity, possibly because it tends to prioritise ICL examples that are most perceptually similar, rather than effectively demonstrating the reasoning process. By fine-tuning the embeddings, we not only harness the potential of heterogeneous multi-modal sensor input but also enable more effective ICL example retrieval.

We also investigate whether to apply ICL examples during training or solely in inference time. As shown in Tab. III, we found that the MLLM is incapable of making reasonable predictions using ICL examples without prior training, regardless of the retrieval strategy chosen; as the model generates random string and non-floating-point number, which precludes the calculation of sensible metrics indicated as N.A in the corresponding entry. This suggests that the pre-trained MLLM is not equipped to effectively perform zero-shot ICL. We hypothesise that supervised fine-tuning plays a crucial role in enhancing the ICL capabilities of MLLM, necessitating the provision of reasoning demonstrations, which aligns with observations in [18].

We further investigate the effect of the number of ICL examples. In particular, we compare the performance using the same optimal hybrid search as above but with a varying number of ICL examples. As shown in Tab. IV, we observe that increasing the number of ICL examples from 1 to 2 improves performance in explanation and justification while slightly decreasing the course control signal accuracy. It is worth noting that the choice of at most two ICL examples is constrained by the MLLM architecture. We include analysis and discussion on this limitation in Sec. V-A.

TABLE I: **Driving Action Explanation and Justification Evaluation.** B4, C, and M represent BLEU4, CIDEr, and METEOR, respectively, for measuring the accuracy and quality of textual driving explanation. The upper part indicates the evaluation on the in-distribution BDD-X test set. The lower part indicates the zero-shot generalisation evaluation on the Spoken-SAX dataset.

Method	Is Generalist?	Action			Justification		
		B4 ↑	C ↑	M ↑	B4 ↑	C ↑	M ↑
<i>In Distribution Performance (BDD-X)</i>							
S2VT [76]		×	30.2	179.8	27.5	6.3	53.4
S2VT++ [76]		×	27.1	157.0	26.4	5.8	52.7
SAA [39]		×	31.8	214.8	29.1	7.1	66.1
WAA [39]		×	32.3	215.8	29.2	7.3	69.5
ADAPT [35]		×	34.6	247.5	30.6	11.4	102.6
DriveGPT4 [81]	✓		30.0	214.0	29.8	9.4	102.7
OURS	✓		34.3	260.8	30.7	11.1	109.1
Δ w.r.t generalist SOTA		+14.3%	+21.9%	+3.0%	+18.1%	+6.2%	+1.4%
<i>Zero-shot Generalisation (Spoken-SAX)</i>							
ADAPT [35]		×	0.0	22.3	26.7	3.1	8.6
Base w/o ICL	✓		0.0	5.7	21.6	2.1	4.7
OURS w ICL	✓		9.9	48.9	27.5	5.6	17.1
Δ w.r.t SOTA		+-%	+119.3%	+3.0%	+80.6%	+98.8%	+17.7%

TABLE II: **Control Signals Prediction Accuracy Evaluation on BDD-X dataset.**

Method	Course						Speed					
	RMSE(degree)↓	A _{0.1} ↑	A _{0.5} ↑	A _{1.0} ↑	A _{5.0} ↑	A _{10.0} ↑	RMSE(m/s)↓	A _{0.1} ↑	A _{0.5} ↑	A _{1.0} ↑	A _{5.0} ↑	A _{10.0} ↑
ADAPT [35]	5.87	54.49	86.39	91.06	97.36	98.20	2.68	11.77	31.79	47.48	92.75	95.87
DriveGPT4 [81]	4.57	69.22	79.14	84.47	95.72	96.74	1.09	56.93	77.77	87.97	99.00	99.57
OURS	4.48	74.32	88.69	93.12	98.30	99.10	0.69	51.12	85.54	94.49	99.81	99.91

TABLE III: **Ablation Study** on Retrieval Strategy and In-Context Learning Phase. Visual and Hybrid Search refers to the use of video embeddings or projected hybrid sensor embeddings, respectively. Training and Inference denote whether in-context learning examples are provided during the corresponding phase.

Retrieval Strategy		ICL Phase				BDD-X				
Visual Search	Hybrid Search	Training	Inference	Act. B4	Act. C	Jus. B4	Jus. C	Speed Err.	Course Err.	
				29.8	222.1	5.9	58.9	0.67	5.61	
✓			✓	0.0	0.0	0.0	0.0	N/A	N/A	
	✓		✓	0.0	0.0	0.0	0.0	N/A	N/A	
✓		✓	✓	31.2	222.1	7.7	83.1	0.78	5.61	
	✓	✓	✓	34.3	260.9	11.1	109.1	0.69	4.48	

TABLE IV: **Ablation Study** on number of in-context learning examples on BDD-X.

No. ICL Examples	Act. B4	Act. C	Jus. B4	Jus. C	Speed Err.	Course Err.
1	33.2	257.2	10.2	99.3	0.75	4.15
2	34.3	260.9	11.1	109.1	0.69	4.48

E. Generalisation Capacity

One of the critical capacities of autonomous systems is to generalise to unseen environments out of its training distribution. However, in the domain of explainable driving, we observe the existing methods are unable to perform such generalisation, which poses challenges for their deployment. As shown in lower part of Tab. I, ADAPT and the base MLLM (i.e., training without ICL) reveal dramatic performance degradation as compared to the in-distribution situation. However, our method leverages ICL learning examples to demonstrate a

significant performance boost with a large margin. Note that even though the memory database is constructed with BDD-X, the RA-ICL can still perform generalisation in a zero-shot manner. This is potentially due to the robustness of the hybrid retrieval process, where samples with less distribution shift can still be selected to serve as effective ICL examples.

F. Fine-tuning Retrieval Engine

While RAG-Driver aims to enhance the model’s generalisability in driving action explanation tasks in a training-free manner through in-context learning, we further investigate the potential to improve the retrieval strategy. Specifically, we further train the retrieval engine with additional target domain data from Spoken-SAX on top of original BDD-X data samples. As shown in Tab. V, we observe a further performance boost in terms of driving action explanation

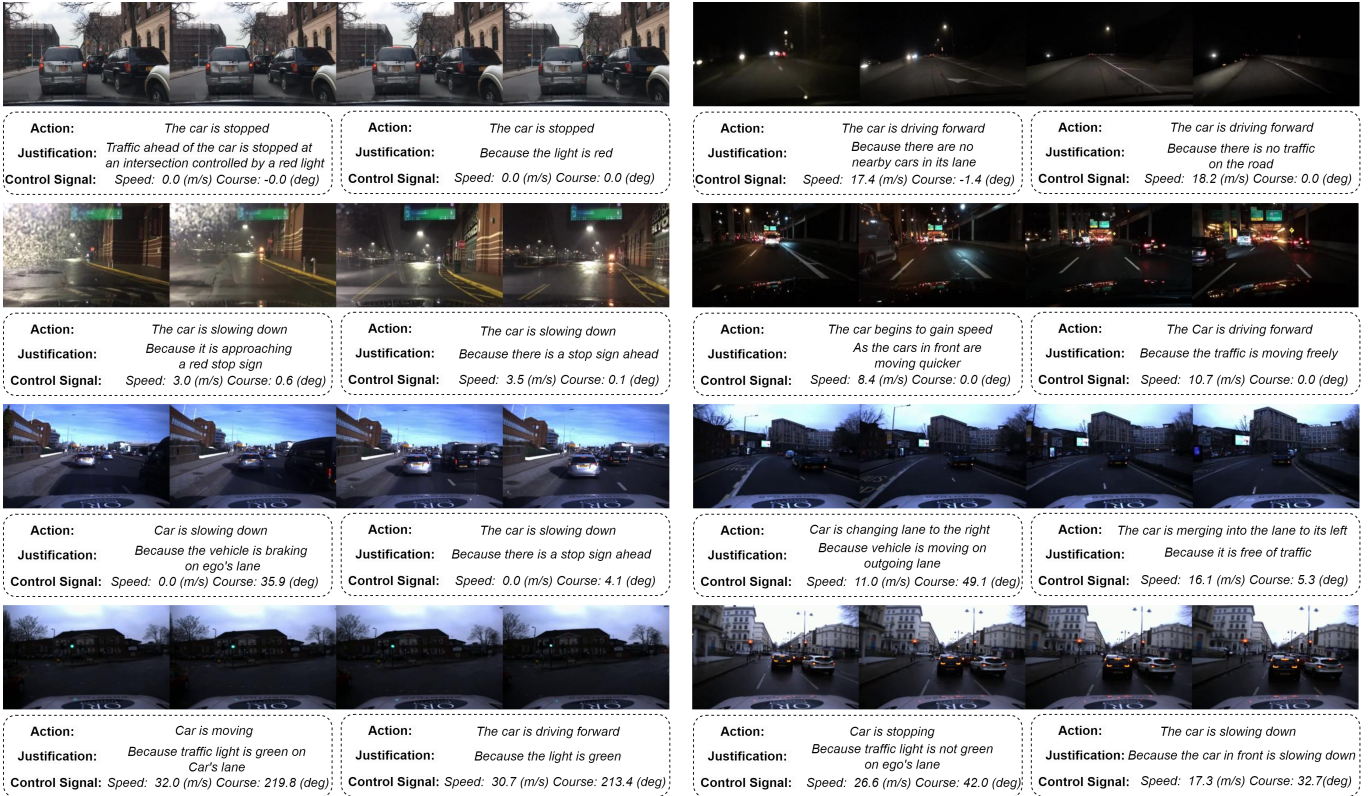


Fig. 5: Qualitative Examples. Comparison between human annotated ground truth (**Left**) and prediction from our method (**Right**) from both BDD-X (**Top 4**) and Spoken-SAX (**Bottom 4**). Each video is downsampled to four frames for visualisation. Despite subtle differences in wording, our method provides driving action explanations and justifications that are comprehensible to humans.

TABLE V: Effect of training retrieval engine with target domain data samples.

Finetune?	BDD-X				Spoken-SAX			
	Act. B4	Act. C	Jus. B4	Jus. C	Act. B4	Act. C	Jus. B3	Jus. C
✗	34.3	260.9	11.1	109.1	9.9	48.9	5.6	17.1
✓	34.7	271.0	10.9	112.4	10.1	52.1	6.7	19.0

and justification in the out-of-distribution setting. Although the improvement in performance is less significant in the in-distribution setting, as indicated by the competing justification metric, the action explanation performance has improved considerably. This suggests a higher potential upper bound for retrieval performance and the potential of learning-based optimization for a better retrieval strategy.

G. Qualitative Demonstration

We also demonstrate a series of qualitative examples comparing the driving action explanation and justification provided by human ground truth and prediction from our method. As shown in Fig. 5, we observe *RAG-Driver* produces robust intelligible action explanation and justification under different environments (i.e. night time and adversarial weather) with a control signal close to the human driver record. More importantly, in the out-of-distribution setting *Spoken-*

SAX as indicated by the clear visual difference, we observe the prediction also produces human-understandable answers, qualitatively validating the exceptional zero-shot generalisation capacity.

V. LIMITATIONS AND FUTURE WORK

This work aims to develop a generalisable explainable driving agent using a Multi-Modal Large Language Model (MLLM), addressing a significant obstacle that has hindered deployment: the poor generalisation capacity. However, as an early exploration, we still observe several limitations that need to be addressed in future works to realize the application of such promising technology.

A. Computational Restriction and Scale of MLLM

While our Multi-modal Large Language Model (MLLM) has shown impressive capabilities in visual reasoning and planning

for driving tasks, it is crucial to note that it consists of only 7 billion parameters. This size is relatively modest compared to more well-known models like GPT-4V [1] and Gemini [71], which have a significantly larger parameter count and exhibit superb performance in visual understanding and reasoning. Although a prominent trend observed in MLLM work is that performance improvements typically occur in tandem with model scaling, and we expect similar advancements in driving applications, we observe this limitation associated with the current model scale.

One of the specific limitations is the number of ICL examples that can be used. During training and inference, we provide two ICL examples for each query. This is due to the limitation of the context window size of the LLM backbone, Vicuna 1.5 [87], which is 4096 tokens. Each additional ICL example introduces roughly an extra 1800 tokens, including a 1024-token fixed-length video sequence and the remaining tokens for language dialogue. While techniques such as Rotary Positional Embeddings (RoPE) [70] and slicing windows can help the model to understand longer contexts, the context window – defining the maximum range of the attention mechanism during a single inference – is fundamentally restricted by the model architecture and remains a bottleneck. We expect the advancement of LLM architectures to support larger context window sizes, enabling a more flexible adoption of ICL examples.

B. Data Scarcity

Another challenge for the application of MLLMs in driving is data scarcity. Observing the trend in the development of MLLMs, their success is largely built upon large-scale pre-training and high-quality data for fine-tuning, which enable more powerful and generalisable models. While the integration of language in the decision-making process of an MLLM-based driving agent significantly enhances explainability and provides a human-understandable interface, it introduces a significant paradigm shift from previous deep learning methods, which reveals a lack of paired driving and language datasets. Currently, the scale of driving-specific video-caption datasets is considerably smaller than its generic counterparts, setting this as the bottleneck for building robust driving agents. Also, the current driving-language dataset mostly contains driving-explanation pairs (e.g., BDD-X [39]), which are not yet suitable for pre-training in terms of scale and language format. However, we observe more emerging works such as DrivingMLM [78] and Reason2Drive [56], which are curating larger scales of well-annotated data specifically for MLLM-based driving applications, providing promising future potential.

C. Hallucination

MLLMs are known to hallucinate, generating information or responses misaligned with facts [31]. While our retrieval-augmented mechanism for grounding the model’s explanations in expert demonstrations has mitigated such phenomena (evident in the much improved Action and Justification explanation metrics in Tab. I), we have observed some isolated failure cases.

For instance, in row 3 column 2 of Fig. 5, the model associates the car’s action of slowing down with the presence of a stop sign, which does not in fact exist. We hypothesise that this is due to the limited capacity of small-scale models which rely on spurious correlations in limited training data. We expect a more powerful backbone model and a more balanced dataset to lead to more faithful predictions and explanations. In the mean time, we would suggest techniques such as real-time verification and rectification [72] for mitigating hallucinations in driving applications as a promising direction.

D. Closed-loop Evaluation

Moreover, the close-loop evaluation in simulator is an important step before the deployment of the MLLM-based driving agent. However, the main obstacle for applying such evaluation in simulator is data scarcity and a significant simulation-to-real gap. While works such as DriveMLM [78] is able to perform the close-form evaluation by specifically trained on large-scale simulation dataset collected in the same CARLA environment, for methods trained on real dataset like RAG-Driver, the adaptation to simulated environment is a non-trivial step. While our method mitigates the effects of distribution shift between real datasets collected in different location and illumination conditions, the larger simulation-to-real gap still remains a significant challenge for closed-loop testing. This in turn highlights the importance of developing more generalisable models for the deployment of the MLLM-based driving agent.

VI. CONCLUSION

We propose *RAG-Driver*, a Multi-Modal Large Language Model with Retrieval-augmented In-context Learning capacity designed for generalisable and explainable end-to-end driving. It exhibits strong capability in providing numerical control signals, along with explanations and justifications for driving actions. More importantly, it shows impressive zero-shot generalisation to unseen environments without the need for additional training.

ACKNOWLEDGEMENT

Jianhao Yuan was supported by a CSC-PAG Oxford Scholarship. Bo Zhao was supported by NSFC-62306046. Lars Kunze and Daniel Omeiza were supported by EPSRC Project RAILS (EP/W011344/1). Matthew Gadd was supported by EPSRC Programme Grant “From Sensing to Collaboration” (EP/V000748/1).

REFERENCES

- [1] Josh Achiam, Steven Adler, Sandhini Agarwal, Lama Ahmad, Ilge Akkaya, Florencia Leoni Aleman, Diogo Almeida, Janko Altenschmidt, Sam Altman, Shyamal Anadkat, et al. GPT-4 technical report. *arXiv preprint arXiv:2303.08774*, 2023.
- [2] Michael Ahn, Anthony Brohan, Noah Brown, Yevgen Chebotar, Omar Cortes, Byron David, Chelsea Finn, Chuyuan Fu, Keerthana Gopalakrishnan, Karol Hausman, et al. Do as I can, not as I say: Grounding language in robotic affordances. *arXiv preprint arXiv:2204.01691*, 2022.
- [3] Jean-Baptiste Alayrac, Jeff Donahue, Pauline Luc, Antoine Miech, Iain Barr, Yana Hasson, Karel Lenc, Arthur Mensch,

- Katherine Millican, Malcolm Reynolds, et al. Flamingo: A visual language model for few-shot learning. *Advances in Neural Information Processing Systems*, 35:23716–23736, 2022.
- [4] Satanjeev Banerjee and Alon Lavie. METEOR: An automatic metric for MT evaluation with improved correlation with human judgments. In *Proceedings of the ACL Workshop on Intrinsic and Extrinsic Evaluation Measures for Machine Translation and/or Summarization*, pages 65–72, 2005.
 - [5] Mariusz Bojarski, Anna Choromanska, Krzysztof Choromanski, Bernhard Firner, Larry Jackel, Urs Muller, and Karol Zieba. VisualBackProp: Efficient visualization of cnns. *arXiv preprint arXiv:1611.05418*, 2016.
 - [6] Mariusz Bojarski, Davide Del Testa, Daniel Dworakowski, Bernhard Firner, Beat Flepp, Prasoon Goyal, Lawrence D Jackel, Mathew Monfort, Urs Muller, Jiakai Zhang, et al. End to end learning for self-driving cars. *arXiv preprint arXiv:1604.07316*, 2016.
 - [7] Mariusz Bojarski, Philip Yeres, Anna Choromanska, Krzysztof Choromanski, Bernhard Firner, Lawrence Jackel, and Urs Muller. Explaining how a deep neural network trained with end-to-end learning steers a car. *arXiv preprint arXiv:1704.07911*, 2017.
 - [8] Jean-François Bonnefon, Azim Shariff, and Iyad Rahwan. The social dilemma of autonomous vehicles. *Science*, 352(6293):1573–1576, 2016.
 - [9] Anthony Brohan, Noah Brown, Justice Carbajal, Yevgen Chebotar, Xi Chen, Krzysztof Choromanski, Tianli Ding, Danny Driess, Avinava Dubey, Chelsea Finn, et al. RT-2: Vision-language-action models transfer web knowledge to robotic control. *arXiv preprint arXiv:2307.15818*, 2023.
 - [10] Tom Brown, Benjamin Mann, Nick Ryder, Melanie Subbiah, Jared D Kaplan, Prafulla Dhariwal, Arvind Neelakantan, Pranav Shyam, Girish Sastry, Amanda Askell, et al. Language models are few-shot learners. *Advances in Neural Information Processing Systems*, 33:1877–1901, 2020.
 - [11] Raphael Chekroun, Marin Toromanoff, Sascha Hornauer, and Fabien Moutarde. GRI: General reinforced imitation and its application to vision-based autonomous driving. *Robotics*, 12(5):127, 2023.
 - [12] Dian Chen, Brady Zhou, Vladlen Koltun, and Philipp Krähenbühl. Learning by cheating. In *Conference on Robot Learning*, pages 66–75. PMLR, 2020.
 - [13] Li Chen, Penghao Wu, Kashyap Chitta, Bernhard Jaeger, Andreas Geiger, and Hongyang Li. End-to-end autonomous driving: Challenges and frontiers. *arXiv preprint arXiv:2306.16927*, 2023.
 - [14] Long Chen, Oleg Sinavski, Jan Hünermann, Alice Karnsund, Andrew James Willmott, Danny Birch, Daniel Maund, and Jamie Shotton. Driving with LLMs: Fusing object-level vector modality for explainable autonomous driving. *arXiv preprint arXiv:2310.01957*, 2023.
 - [15] Kashyap Chitta, Aditya Prakash, and Andreas Geiger. NEAT: Neural attention fields for end-to-end autonomous driving. In *Proceedings of the IEEE/CVF International Conference on Computer Vision*, pages 15793–15803, 2021.
 - [16] Kashyap Chitta, Aditya Prakash, Bernhard Jaeger, Zehao Yu, Katrin Renz, and Andreas Geiger. TransFuser: Imitation with transformer-based sensor fusion for autonomous driving. *IEEE Transactions on Pattern Analysis and Machine Intelligence*, 2022.
 - [17] Damai Dai, Yutao Sun, Li Dong, Yaru Hao, Zhifang Sui, and Furu Wei. Why can GPT learn in-context? language models secretly perform gradient descent as meta optimizers. *arXiv preprint arXiv:2212.10559*, 2022.
 - [18] Qingxiu Dong, Lei Li, Damai Dai, Ce Zheng, Zhiyong Wu, Baobao Chang, Xu Sun, Jingjing Xu, and Zhifang Sui. A survey for in-context learning. *arXiv preprint arXiv:2301.00234*, 2022.
 - [19] Alexey Dosovitskiy, Lucas Beyer, Alexander Kolesnikov, Dirk Weissenborn, Xiaohua Zhai, Thomas Unterthiner, Mostafa Dehghani, Matthias Minderer, Georg Heigold, Sylvain Gelly, et al. An image is worth 16x16 words: Transformers for image recognition at scale. *arXiv preprint arXiv:2010.11929*, 2020.
 - [20] Danny Driess, Fei Xia, Mehdi SM Sajjadi, Corey Lynch, Aakanksha Chowdhery, Brian Ichter, Ayzaan Wahid, Jonathan Tompson, Quan Vuong, Tianhe Yu, et al. PaLM-e: An embodied multimodal language model. *arXiv preprint arXiv:2303.03378*, 2023.
 - [21] Asif Faisal, Md Kamruzzaman, Tan Yigitcanlar, and Graham Currie. Understanding autonomous vehicles. *Journal of Transport and Land Use*, 12(1):45–72, 2019.
 - [22] Matthew Gadd, Daniele De Martini, Letizia Marchegiani, Paul Newman, and Lars Kunze. Sense–assess–explain (sax): Building trust in autonomous vehicles in challenging real-world driving scenarios. In *2020 IEEE Intelligent Vehicles Symposium (IV)*, pages 150–155. IEEE, 2020.
 - [23] Siavash Golkar, Mariel Pettee, Michael Eickenberg, Alberto Bietti, Miles Cranmer, Geraud Krawezik, Francois Lanusse, Michael McCabe, Ruben Ohana, Liam Parker, et al. xVal: A continuous number encoding for large language models. *arXiv preprint arXiv:2310.02989*, 2023.
 - [24] Ishaaan Gulrajani and David Lopez-Paz. In search of lost domain generalization. *arXiv preprint arXiv:2007.01434*, 2020.
 - [25] Wencheng Han, Dongqian Guo, Cheng-Zhong Xu, and Jianbing Shen. DME-Driver: Integrating human decision logic and 3D scene perception in autonomous driving. *arXiv preprint arXiv:2401.03641*, 2024.
 - [26] Jeffrey Hawke, Richard Shen, Corina Gurau, Siddharth Sharma, Daniele Reda, Nikolay Nikolov, Przemysław Mazur, Sean Micklithwaite, Nicolas Griffiths, Amar Shah, et al. Urban driving with conditional imitation learning. In *International Conference on Robotics and Automation (ICRA)*, pages 251–257. IEEE, 2020.
 - [27] Muyang He, Yixin Liu, Boya Wu, Jianhao Yuan, Yueze Wang, Tiejun Huang, and Bo Zhao. Efficient multimodal learning from data-centric perspective. *arXiv preprint arXiv:2402.11530*, 2024.
 - [28] Dan Hendrycks and Kevin Gimpel. Gaussian error linear units (GELUs). *arXiv preprint arXiv:1606.08415*, 2016.
 - [29] Elad Hoffer and Nir Ailon. Deep metric learning using triplet network. In *Similarity-Based Pattern Recognition: Third International Workshop, SIMBAD*, pages 84–92. Springer, 2015.
 - [30] Yihan Hu, Jiazhui Yang, Li Chen, Keyu Li, Chonghao Sima, Xizhou Zhu, Sisiqi Chai, Senyao Du, Tianwei Lin, Wenhui Wang, Lewei Lu, Xiaosong Jia, Qiang Liu, Jifeng Dai, Yu Qiao, and Hongyang Li. Planning-oriented autonomous driving. In *Proceedings of the IEEE/CVF Conference on Computer Vision and Pattern Recognition (CVPR)*, pages 17853–17862, June 2023.
 - [31] Lei Huang, Weijiang Yu, Weitao Ma, Weihong Zhong, Zhangyin Feng, Haotian Wang, Qianglong Chen, Weihua Peng, Xiaocheng Feng, Bing Qin, et al. A survey on hallucination in large language models: Principles, taxonomy, challenges, and open questions. *arXiv preprint arXiv:2311.05232*, 2023.
 - [32] Siyuan Huang, Zhengkai Jiang, Hao Dong, Yu Qiao, Peng Gao, and Hongsheng Li. Instruct2Act: Mapping multi-modality instructions to robotic actions with large language model. *arXiv preprint arXiv:2305.11176*, 2023.
 - [33] Bernhard Jaeger, Kashyap Chitta, and Andreas Geiger. Hidden biases of end-to-end driving models. *arXiv preprint arXiv:2306.07957*, 2023.
 - [34] Kanishk Jain, Varun Chhangani, Amogh Tiwari, K Madhava Krishna, and Vineet Gandhi. Ground then navigate: Language-guided navigation in dynamic scenes. In *International Conference on Robotics and Automation (ICRA)*, pages 4113–4120. IEEE, 2023.
 - [35] Bu Jin, Xinyu Liu, Yupeng Zheng, Pengfei Li, Hao Zhao, Tong Zhang, Yuhang Zheng, Guyue Zhou, and Jingjing Liu.

- Adapt: Action-aware driving caption transformer. *arXiv preprint arXiv:2302.00673*, 2023.
- [36] Nikhil Kandpal, Haikang Deng, Adam Roberts, Eric Wallace, and Colin Raffel. Large language models struggle to learn long-tail knowledge. In *International Conference on Machine Learning*, pages 15696–15707. PMLR, 2023.
- [37] Alex Kendall, Jeffrey Hawke, David Janz, Przemyslaw Mazur, Daniele Reda, John-Mark Allen, Vinh-Dieu Lam, Alex Bewley, and Amar Shah. Learning to drive in a day. In *International Conference on Robotics and Automation (ICRA)*, pages 8248–8254. IEEE, 2019.
- [38] Jinkyu Kim and John Canny. Interpretable learning for self-driving cars by visualizing causal attention. In *Proceedings of the IEEE International Conference on Computer Vision and Pattern Recognition*, pages 2942–2950, 2017.
- [39] Jinkyu Kim, Anna Rohrbach, Trevor Darrell, John Canny, and Zeynep Akata. Textual explanations for self-driving vehicles. *Proceedings of the European Conference on Computer Vision (ECCV)*, 2018.
- [40] James Kirkpatrick, Razvan Pascanu, Neil Rabinowitz, Joel Veness, Guillaume Desjardins, Andrei A Rusu, Kieran Milan, John Quan, Tiago Ramalho, Agnieszka Grabska-Barwinska, et al. Overcoming catastrophic forgetting in neural networks. *Proceedings of the National Academy of Sciences*, 114(13):3521–3526, 2017.
- [41] Soroush Abbasi Koohpayegani and Hamed Pirsiavash. SimA: Simple softmax-free attention for vision transformers. In *Proceedings of the IEEE/CVF Winter Conference on Applications of Computer Vision*, pages 2607–2617, 2024.
- [42] Patrick Lewis, Ethan Perez, Aleksandra Piktus, Fabio Petroni, Vladimir Karpukhin, Naman Goyal, Heinrich Küttler, Mike Lewis, Wen-tau Yih, Tim Rocktäschel, et al. Retrieval-augmented generation for knowledge-intensive NLP tasks. *Advances in Neural Information Processing Systems*, 33:9459–9474, 2020.
- [43] Junnan Li, Dongxu Li, Silvio Savarese, and Steven Hoi. Blip-2: Bootstrapping language-image pre-training with frozen image encoders and large language models. *arXiv preprint arXiv:2301.12597*, 2023.
- [44] Quanyi Li, Zhenghao Peng, and Bolei Zhou. Efficient learning of safe driving policy via human-AI copilot optimization. *arXiv preprint arXiv:2202.10341*, 2022.
- [45] Zhihao Li, Toshiyuki Motoyoshi, Kazuma Sasaki, Tetsuya Ogata, and Shigeki Sugano. Rethinking self-driving: Multi-task knowledge for better generalization and accident explanation ability. *arXiv preprint arXiv:1809.11100*, 2018.
- [46] Bin Lin, Bin Zhu, Yang Ye, Munan Ning, Peng Jin, and Li Yuan. Video-LLaVA: Learning united visual representation by alignment before projection. *arXiv preprint arXiv:2311.10122*, 2023.
- [47] Kevin Lin, Christopher Agia, Toki Migimatsu, Marco Pavone, and Jeannette Bohg. Text2Motion: From natural language instructions to feasible plans. *arXiv preprint arXiv:2303.12153*, 2023.
- [48] Haotian Liu, Chunyuan Li, Qingyang Wu, and Yong Jae Lee. Visual instruction tuning. *Advances in Neural Information Processing Systems*, 2023.
- [49] Huashao Luo, Lei Ji, Ming Zhong, Yang Chen, Wen Lei, Nan Duan, and Tianrui Li. CLIP4Clip: An empirical study of clip for end to end video clip retrieval. *arXiv preprint arXiv:2104.08860*, 2021.
- [50] Ruipu Luo, Ziwing Zhao, Min Yang, Junwei Dong, Minghui Qiu, Pengcheng Lu, Tao Wang, and Zhongyu Wei. Valley: Video assistant with large language model enhanced abilitY. *arXiv preprint arXiv:2306.07207*, 2023.
- [51] Yingzi Ma, Yulong Cao, Jiachen Sun, Marco Pavone, and Chaowei Xiao. Dolphins: Multimodal language model for driving. *arXiv preprint arXiv:2312.00438*, 2023.
- [52] Yunsheng Ma, Can Cui, Xu Cao, Wenqian Ye, Peiran Liu, Juanwu Lu, Amr Abdelraouf, Rohit Gupta, Kyungtae Han, Aniket Bera, et al. LaMPilot: An open benchmark dataset for autonomous driving with language model programs. *arXiv preprint arXiv:2312.04372*, 2023.
- [53] Jiageng Mao, Junjie Ye, Yuxi Qian, Marco Pavone, and Yue Wang. A language agent for autonomous driving. *arXiv preprint arXiv:2311.10813*, 2023.
- [54] Ana-Maria Marcu, Long Chen, Jan Hünermann, Alice Karnsund, Benoit Hanotte, Prajwal Chidananda, Saurabh Nair, Vijay Badrinarayanan, Alex Kendall, Jamie Shotton, et al. Lingoqa: Video question answering for autonomous driving. *arXiv preprint arXiv:2312.14115*, 2023.
- [55] Keisuke Mori, Hiroshi Fukui, Takuya Murase, Tsubasa Hirakawa, Takayoshi Yamashita, and Hironobu Fujiyoshi. Visual explanation by attention branch network for end-to-end learning-based self-driving. In *Intelligent Vehicles Symposium (IV)*, pages 1577–1582, 2019. doi: 10.1109/IVS.2019.8813900.
- [56] Ming Nie, Renyuan Peng, Chunwei Wang, Xinyue Cai, Jianhua Han, Hang Xu, and Li Zhang. Reason2Drive: Towards interpretable and chain-based reasoning for autonomous driving. *arXiv preprint arXiv:2312.03661*, 2023.
- [57] Daniel Omeiza, Helena Webb, Marina Jirocka, and Lars Kunze. Explanations in autonomous driving: A survey. *IEEE Transactions on Intelligent Transportation Systems*, 23(8):10142–10162, 2022. doi: 10.1109/TITS.2021.3122865.
- [58] Abhishek Padalkar, Acorn Pooley, Ajinkya Jain, Alex Bewley, Alex Herzog, Alex Irpan, Alexander Khazatsky, Anant Rai, Anikait Singh, Anthony Brohan, et al. Open X-Embodiment: Robotic Learning Datasets and RT-X Models. *arXiv preprint arXiv:2310.08864*, 2023.
- [59] Kishore Papineni, Salim Roukos, Todd Ward, and Wei-Jing Zhu. Bleu: A method for automatic evaluation of machine translation. In *Proceedings of the 40th annual meeting of the Association for Computational Linguistics*, pages 311–318, 2002.
- [60] Zhenghao Peng, Wenjie Mo, Chenda Duan, Quanyi Li, and Bolei Zhou. Learning from active human involvement through proxy value propagation. In *Thirty-seventh Conference on Neural Information Processing Systems*, 2023.
- [61] Dean A Pomerleau. Alvinn: An autonomous land vehicle in a neural network. *Advances in Neural Information Processing Systems*, 1, 1988.
- [62] Krishan Rana, Jesse Haviland, Sourav Garg, Jad Abou-Chakra, Ian Reid, and Niko Suenderhauf. SayPlan: Grounding large language models using 3d scene graphs for scalable task planning. *arXiv preprint arXiv:2307.06135*, 2023.
- [63] Katrin Renz, Kashyap Chitta, Otniel-Bogdan Mercea, A Koepke, Zeynep Akata, and Andreas Geiger. PlanT: Explainable planning transformers via object-level representations. *arXiv preprint arXiv:2210.14222*, 2022.
- [64] Ohad Rubin, Jonathan Herzig, and Jonathan Berant. Learning to retrieve prompts for in-context learning. *arXiv preprint arXiv:2112.08633*, 2021.
- [65] Abbas Sadat, Sergio Casas, Mengye Ren, Xinyu Wu, Pranaab Dhawan, and Raquel Urtasun. Perceive, predict, and plan: Safe motion planning through interpretable semantic representations. In *Proceedings of the European Conference on Computer Vision (ECCV)*, pages 414–430. Springer, 2020.
- [66] Wilko Schwarting, Javier Alonso-Mora, and Daniela Rus. Planning and decision-making for autonomous vehicles. *Annual Review of Control, Robotics, and Autonomous Systems*, 2018.
- [67] Hao Sha, Yao Mu, Yuxuan Jiang, Li Chen, Chenfeng Xu, Ping Luo, Shengbo Eben Li, Masayoshi Tomizuka, Wei Zhan, and Mingyu Ding. LanguageMPC: Large language models as decision makers for autonomous driving. *arXiv preprint arXiv:2310.03026*, 2023.
- [68] Hao Shao, Letian Wang, Ruobing Chen, Hongsheng Li, and

- Yu Liu. Safety-enhanced autonomous driving using interpretable sensor fusion transformer. In *Conference on Robot Learning*, pages 726–737. PMLR, 2023.
- [69] SP Sharan, Francesco Pittaluga, Manmohan Chandraker, et al. LLM-Assist: Enhancing closed-loop planning with language-based reasoning. *arXiv preprint arXiv:2401.00125*, 2023.
- [70] Jianlin Su, Murtadha Ahmed, Yu Lu, Shengfeng Pan, Wen Bo, and Yunfeng Liu. Roformer: Enhanced transformer with rotary position embedding. *Neurocomputing*, 568:127063, 2024.
- [71] Gemini Team, Rohan Anil, Sebastian Borgeaud, Yonghui Wu, Jean-Baptiste Alayrac, Jiahui Yu, Radu Soricut, Johan Schalkwyk, Andrew M Dai, Anja Hauth, et al. Gemini: A family of highly capable multimodal models. *arXiv preprint arXiv:2312.11805*, 2023.
- [72] SM Tonmoy, SM Zaman, Vinija Jain, Anku Rani, Vipula Rawte, Aman Chadha, and Amitava Das. A comprehensive survey of hallucination mitigation techniques in large language models. *arXiv preprint arXiv:2401.01313*, 2024.
- [73] Marin Toromanoff, Emilie Wirbel, and Fabien Moutarde. End-to-end model-free reinforcement learning for urban driving using implicit affordances. In *Proceedings of the IEEE/CVF Conference on Computer Vision and Pattern Recognition*, pages 7153–7162, 2020.
- [74] Hugo Touvron, Louis Martin, Kevin Stone, Peter Albert, Amjad Almahairi, Yasmine Babaei, Nikolay Bashlykov, Soumya Batra, Prajjwal Bhargava, Shruti Bhosale, et al. Llama 2: Open foundation and fine-tuned chat models. *arXiv preprint arXiv:2307.09288*, 2023.
- [75] Ramakrishna Vedantam, C Lawrence Zitnick, and Devi Parikh. CIDEr: Consensus-based image description evaluation. In *Proceedings of the IEEE Conference on Computer Vision and Pattern Recognition*, pages 4566–4575, 2015.
- [76] Subhashini Venugopalan, Marcus Rohrbach, Jeffrey Donahue, Raymond Mooney, Trevor Darrell, and Kate Saenko. Sequence to sequence-video to text. In *Proceedings of the IEEE/CVF International Conference on Computer Vision*, pages 4534–4542, 2015.
- [77] Hengli Wang, Peide Cai, Rui Fan, Yuxiang Sun, and Ming Liu. End-to-end interactive prediction and planning with optical flow distillation for autonomous driving. In *Proceedings of the IEEE/CVF Conference on Computer Vision and Pattern Recognition*, pages 2229–2238, 2021.
- [78] Wenhui Wang, Jiangwei Xie, ChuanYang Hu, Haoming Zou, Jianan Fan, Wenwen Tong, Yang Wen, Silei Wu, Hanming Deng, Zhiqi Li, et al. DriveMLM: Aligning multi-modal large language models with behavioral planning states for autonomous driving. *arXiv preprint arXiv:2312.09245*, 2023.
- [79] Jerry Wei, Le Hou, Andrew Lampinen, Xiangning Chen, Da Huang, Yi Tay, Xinyun Chen, Yifeng Lu, Denny Zhou, Tengyu Ma, et al. Symbol tuning improves in-context learning in language models. *arXiv preprint arXiv:2305.08298*, 2023.
- [80] Yi Xiao, Felipe Codevilla, Diego Porres Bustamante, and Antonio M Lopez. Scaling self-supervised end-to-end driving with multi-view attention learning. *arXiv preprint arXiv:2302.03198*, 2023.
- [81] Zhenhua Xu, Yujia Zhang, Enze Xie, Zhen Zhao, Yong Guo, Kenneth KY Wong, Zhenguo Li, and Hengshuang Zhao. DriveGPT4: Interpretable end-to-end autonomous driving via large language model. *arXiv preprint arXiv:2310.01412*, 2023.
- [82] Zhenjie Yang, Xiaosong Jia, Hongyang Li, and Junchi Yan. A survey of large language models for autonomous driving. *arXiv preprint arXiv:2311.01043*, 2023.
- [83] Éloi Zablocki, Hédi Ben-Younes, Patrick Pérez, and Matthieu Cord. Explainability of deep vision-based autonomous driving systems: Review and challenges. *International Journal of Computer Vision*, 130(10):2425–2452, 2022.
- [84] Wenyuan Zeng, Wenjie Luo, Simon Suo, Abbas Sadat, Bin Yang, Sergio Casas, and Raquel Urtasun. End-to-end interpretable neural motion planner. In *Proceedings of the IEEE/CVF Conference on Computer Vision and Pattern Recognition*, pages 8660–8669, 2019.
- [85] Hang Zhang, Xin Li, and Lidong Bing. Video-llama: An instruction-tuned audio-visual language model for video understanding. *arXiv preprint arXiv:2306.02858*, 2023.
- [86] Qihang Zhang, Zhenghao Peng, and Bolei Zhou. Learning to drive by watching YouTube videos: Action-conditioned contrastive policy pretraining. In *European Conference on Computer Vision*, pages 111–128. Springer, 2022.
- [87] Lianmin Zheng, Wei-Lin Chiang, Ying Sheng, Siyuan Zhuang, Zhanghao Wu, Yonghao Zhuang, Zi Lin, Zhuohan Li, Dacheng Li, Eric Xing, et al. Judging LLM-as-a-Judge with MT-Bench and Chatbot Arena. *arXiv preprint arXiv:2306.05685*, 2023.
- [88] Bin Zhu, Bin Lin, Munan Ning, Yang Yan, Jiaxi Cui, HongFa Wang, Yatian Pang, Wenhao Jiang, Junwu Zhang, Zongwei Li, et al. LanguageBind: Extending video-language pretraining to n-modality by language-based semantic alignment. *arXiv preprint arXiv:2310.01852*, 2023.
- [89] Deyao Zhu, Jun Chen, Xiaoqian Shen, Xiang Li, and Mohamed Elhoseiny. MiniGPT-4: Enhancing vision-language understanding with advanced large language models. *arXiv preprint arXiv:2304.10592*, 2023.

APPENDIX

A. Training Details

Embedding Projector We leverage a three-layer MLP as the embedding projector to fuse the video 1×1024 and control signal 1×28 embedding into a hybrid embedding. The architecture of the lightweight projector is a four-layer MLP with GELU activation. It has an input dimension of 1052 and an output dimension of 1024. The margin used in triplet loss is 0.5. We train the model for 200 epochs with a learning rate of $1e-5$ with Adam optimiser.

MLLM Backbone We use a learning rate of $2e-5$ with a cosine scheduler. We use a batch size of 4 with a gradient accumulation step of 2 on 8 *A100 GPUs*, which leads to an effective training batch size of 128. We use a warm-up strategy in the first 5 epochs with a warm-up ratio of 0.03. We train the model for 2 epochs.

B. Baseline Details

In our comparison, we evaluate several baseline methods. The first, S2VT [76], utilises an end-to-end sequence-to-sequence model with Long Short-Term Memory (LSTM) networks. It is trained on paired video-sentence data, linking video frame sequences to corresponding word sequences, enabling it to generate descriptive captions for video events. The second method, WAA [39], employs a visual attention model that trains a convolutional network from images to vehicle control commands. This method focuses on identifying influential image regions through the controller’s attention and uses an attention-based video-to-text model to produce textual explanations aligned with the controller’s attention maps, grounding the explanations in relevant scene parts. The third approach, ADAPT [35], is a transformer-based method that leverages a multi-task joint training framework. It aligns driving action captioning with control signal prediction tasks. Finally, DriveGPT4 [81], trained using LLaVA [48] to generate a visual instruction tuning dataset derived from the BDD-X dataset [39], processes multimodal input data and is capable of generating text responses while predicting control signals, fine-tuned with the assistance of ChatGPT on the new dataset.

C. Linear Layer Parameter Update Derivations

Consider a forward-pass through a linear layer \mathcal{F} after its weights W_0 have been updated by ΔW

$$\mathbf{y} = \mathcal{F}(\mathbf{x}) = (W_0 + \Delta W)\mathbf{x} = W_0\mathbf{x} + \Delta W\mathbf{x}$$

The weight update itself is expressed as

$$\Delta W = \eta \frac{\partial L}{\partial \mathbf{y}}|_{\mathbf{y}_i} \mathbf{x}_i^T \Rightarrow \Delta W\mathbf{x} = \eta \frac{\partial L}{\partial \mathbf{y}}|_{\mathbf{y}_i} \mathbf{x}_i^T \mathbf{x}$$

where $\mathbf{x}_i, \mathbf{y}_i$ are the input and output to the layer that resulted in the weight update. Now, if we in fact have optimised over a mini-batch of input-outputs $\mathbf{x}_i, \mathbf{y}_i$ we have

$$\Delta W = \sum_i \eta \frac{\partial L}{\partial \mathbf{y}}|_{\mathbf{y}_i} \mathbf{x}_i^T \Rightarrow \Delta W\mathbf{x} = \sum_i \eta \frac{\partial L}{\partial \mathbf{y}}|_{\mathbf{y}_i} \mathbf{x}_i^T \mathbf{x}$$

Therefore we have a weighted sum of dot products, which is akin to an attention mechanism. Indeed, from Eq. (5) we can apply *softmax-free* linear attention expressions such as in [41] for

$$W_V[\mathbf{z}_{icl}; \mathbf{z}_q] \text{softmax} \left(\frac{(W_K \mathbf{z}_{1:n})^T (W_Q \mathbf{z}_{1:n})}{\sqrt{d^i}} \right) \\ \rightarrow W_V[\mathbf{z}_{icl}; \mathbf{z}_q] (W_K[\mathbf{z}_{icl}; \mathbf{z}_q])^T W_Q \mathbf{z}_{1:n}$$

Multiplying the linear attention matrices through the stacked in-context and query embeddings we have

$$W_V \mathbf{z}_{icl} (W_K \mathbf{z}_{icl})^T W_Q \mathbf{z}_{1:n} + W_V \mathbf{z}_q (W_K \mathbf{z}_q)^T W_Q \mathbf{z}_{1:n}$$

Now take out a common factor of $W_Q \mathbf{z}_{1:n}$ for

$$(W_V \mathbf{z}_{icl} (W_K \mathbf{z}_{icl})^T + W_V \mathbf{z}_q (W_K \mathbf{z}_q)^T) W_Q \mathbf{z}_{1:n}$$

and put $\Delta W_{ICL} = W_V \mathbf{z}_{icl} (W_K \mathbf{z}_{icl})^T$ and $W_{ZSL} = W_V \mathbf{z}_q (W_K \mathbf{z}_q)^T$ as the terms both pre-multiplying $W_Q \mathbf{z}_{1:n}$. Note that W_{ZSL} is *independent of the in-context terms* (depending only on the query). Now, in ΔW_{ICL} we in fact have a set of in-context retrieved samples $\mathbf{z}_{icl,i}$ such that

$$W_V[\mathbf{z}_{icl,0}, \mathbf{z}_{icl,1}, \dots] (W_K[\mathbf{z}_{icl,0}, \mathbf{z}_{icl,1}, \dots])^T \\ \rightarrow \Delta W_{ICL} = \sum_i W_V \mathbf{z}_{icl,i} (W_K \mathbf{z}_{icl,i})^T$$

Finally, by inspection of similar dot-product expressions $W_V \mathbf{z}_{icl,i} (W_K \mathbf{z}_{icl,i})^T \leftrightarrow \eta \frac{\partial L}{\partial \mathbf{y}}|_{\mathbf{y}_i} \mathbf{x}_i^T \mathbf{x}$ we note that we match the form for the linear layer above

$$(W_{ZSL} + \Delta W_{ICL}) W_Q \mathbf{z}_{1:n} \leftrightarrow (W + \Delta W) \mathbf{x}$$

This can therefore be interpreted to say that the output of the attention is adjusted in a meta-optimal way to conform to the samples provided as input context, much like gradient descent on the linear layer would adjust that layer to conform to the mini-batch training data, but *crucially* in the case of *RAG-Driver*, without supervision.

D. Action Representation

One potential future research direction is action representation. In our study, we adopted a floating-point number action representation for two main reasons: (1) its validated effectiveness in related research such as robot manipulation (e.g., RT-2 [9], RT-X [58]) and driving applications (e.g., DriveGPT4 [81]); (2) its intuitive alignment with human understanding. However, general-purpose LLMs are known for their suboptimal performance in predicting floating-point numbers [23]. We hypothesise that this is due to the discontinuous encoding of real numbers when represented as language tokens, where such representation does not adhere to the linearity of real number space regarding addition and multiplication. Although our approach involves fine-tuning the numerical language tokens with a paired visual-language-action dataset, known as symbol tuning [79], to mitigate this issue, we consider the exploration of alternative methods such as continuous number representation [23] and intermediate controller input [67] for action representation as a promising avenue for future research.